Critical-state model for harmonic generation in high-temperature superconductors

L. Ji, R. H. Sohn, G. C. Spalding, C. J. Lobb, and M. Tinkham
Department of Physics and Division of Applied Sciences, Harvard University, Cambridge, Massachusetts 02138
(Received 16 June 1989)

High-temperature superconductors exhibit harmonic generation when immersed in an ac magnetic field. To explain this phenomenon, we propose a macroscopic critical-state model as an alternative to the loop model used by Jeffries *et al.* While the original Bean model of the critical state only predicts odd harmonics, our extended model also predicts even harmonics by taking into account the dependence of the critical current upon magnetic field. The results of our measurements of harmonic signals as a function of ac magnetic field, dc magnetic field, temperature, and harmonic number are consistent with the proposed model. In particular, we find that, as the magnetic field is increased, the critical current crosses over from the Bean regime, where J_c is independent of field, to the Anderson-Kim regime, where J_c is approximately inversely proportional to the field.

I. INTRODUCTION

A type-II superconductor will generate higher-harmonic components of magnetization when immersed in an ac magnetic field. These phenomena were studied extensively by Bean, who used a critical-state model to explain them;[1] only odd harmonics were reported for conventional superconductors even in the presence of nonzero dc magnetic fields. Similar experiments have been performed more recently on high-temperature superconductors. It is found that these superconductors, whether they are in the form of bulk ceramics, powders, or single crystals, also generate higher harmonics.[2-6] Only odd harmonics are generated in a pure ac field, while in the presence of an additional dc field, even harmonics are also generated. To explain these phenomena in high-temperature superconductors, various theoretical models have been proposed, such as the inverse Josephson effect,[2] quantized loops with weak links,[3,4] and the loop model with phase slips.[7] However, in addition to using questionable physical assumptions, none of these models can account for all of the experimental aspects of harmonic generation in high-temperature superconductors.

In this paper, we extend our earlier work[6] based on the macroscopic critical-state model and develop an analytical solution which accounts naturally for odd- and even-harmonic generation in high-temperature superconductors. The generation of even harmonics arises from a strong field dependence of the critical current in high-T_c materials, even at very small fields. We also report measurements of the harmonic amplitudes as a function of ac magnetic field, dc magnetic field, temperature, and harmonic number. By measuring harmonic power, we observed that as the magnetic field is increased, the critical current crosses over from the Bean regime,[1] where J_c is taken to be independent of field, to the Anderson-Kim[8] regime, where J_c is taken to be inversely proportional to the field. Generation of even harmonics only occurs in the latter case.

II. MATERIALS AND PROCEDURE

The high-temperature superconductors used in our experiments are bulk and powder samples of $YBa_2Cu_3O_7$ obtained both commercially[9] and through synthesis in our lab. Using ac fields of up to 10 G in our experiments, we observed strong harmonic generation in powders (average size about 100 μm) and bulk ceramics, while weaker harmonic signals were seen at 77 K in our higher-grade bulk ceramics. We attribute this difference to the fact that the higher-grade materials have higher critical currents, so that the fields used in our experiments were insufficient to drive the samples into the region where harmonic generation is readily observable.

The apparatus used in our experiments is similar to those used in making mutual inductance ac susceptibility measurements. A function generator (500 Hz to 50 kHz) supplies an ac current to a primary coil to produce a field $H_{ac}\cos(\omega t)$. The current is measured by monitoring the voltage across a 2-Ω resistor connected in series with the coil. Inside the primary coil is a secondary coil of 80 turns which encloses the sample and is connected in series with an identical coil counterwound and positioned to give a zero net signal when the sample is absent. The output of the secondary coils, which is proportional to the time derivative of the magnetization, is connected to a Hewlett-Packard 3561A dynamic signal analyzer. Another coil coaxial to the primary coil is used to produce dc fields.

We also measured hysteresis loops for the samples using an oscilloscope. The x axis of the scope is connected to voltage across the 2Ω resistor which is proportional to the ac drive field, and the y axis of the scope is connected to an integrated version of the secondary coil output, which is proportional to the magnetization.

III. CRITICAL-STATE MODEL

The critical-state model proposed by Bean[1] provides a mechanism for harmonic generation in type-II superconductors. For simplicity, it was originally assumed by

Bean that J_c is constant in the critical state, but this leads to the generation of only odd harmonics. Now we will show that a generalized critical-state model with $J_c(H)$ predicts the generation of both odd and even harmonics in the presence of an additional dc field.

The central idea of the critical-state model is[1] "there exists a limiting macroscopic superconducting current density $J_c = J_c(H)$ that a hard superconductor can carry and, further, that any electromotive force, however small, will induce this full current to flow locally. On this picture only three states of current flow are possible with a given axis of magnetic field: zero current for those regions that have never felt the magnetic field and full current flow perpendicular to the field axis, the sense depending on the sense of the electromagnetic force that accompanied the last local change of field." The average magnetization induced by a given external field can be calculated by averaging the local flux density. We note that this model does not require the critical current to be constant, and that in general J_c does depend on the local field.

When a superconductor is immersed in a pure ac field $H = H_{ac}\cos(\omega t)$, we have $M(\omega t) = -M(\omega t + \pi)$, since J_c only depends on $|H|$ which is the same for ωt and $\omega t + \pi$. Since

$$\sin(n\omega t) = (-1)^n \sin[n(\omega t + \pi)]$$

and

$$\cos(n\omega t) = (-1)^n \cos[n(\omega t + \pi)] ,$$

an $M(\omega t)$ having this symmetry (of only changing sign when $\omega t \rightarrow \omega t + \pi$) can contain only odd n harmonics. Now if we apply a dc field in addition to the ac field, then J_c at

$$H = H_{dc} + H_{ac}\cos(\omega t)$$

will *not* be equal to J_c at

$$H = H_{dc} + H_{ac}\cos(\omega t + \pi)$$

because J_c depends on $|H|$. Therefore the generalized critical-state model with $J_c(H)$ allows the generation of even harmonics in the presence of a dc field.

The generation of even harmonics has not been reported in conventional superconductors. The probable reason is that in order for this generation to be prominent, the following conditions must be satisfied: (1) the critical current is field dependent, (2) the dc and ac fields are of the same order of magnitude, and (3) the total field is much greater than H_{c1}. Since H_{c1} is rather large for conventional materials except near T_c, the generation of even harmonics may not be observable with the rather small ac field amplitudes typically used in this type of experiment. In high-T_c superconductors, the lower critical field H_{c1J} of the effective medium[10] (defined as the minimum field for flux to penetrate *between* the grains) is about 1 Oe (or even less if the intergranular coupling is weaker), so that the generation of both even and odd harmonics occurs at more convenient fields.

Now we present an analytical solution based on the critical-state model. First we discuss the Bean model where J_c is taken to be constant. Then we discuss the case where J_c is taken to be field dependent. Work by Anderson and Kim and coworkers[8] shows that taking J_c to be proportional to the inverse of H is a good approximation for the critical state. This case will be called the "Anderson-Kim model." Before going into the algebraic details of the two models, we point out that *any* field dependence in J_c, such as J_c proportional to $\exp(-\zeta H)$ for example, will also lead to the generation of both even and odd harmonics. Therefore the Anderson-Kim model is only a simple example with which the essence of the underlying physics can be seen.

A. Bean model

The critical current can be taken to be more or less constant in two cases: (1) when the total field is small, and (2) over a subloop which is small and far away from $H = 0$, so that the fractional change in H is small.

The assumption that J_c is constant leads to a straight line flux density profile. For a sample of a given size, there exists a minimum field H^* to penetrate the whole sample. For an infinitely long slab of thickness D and an infinitely long cylinder of radius R, this size-dependent penetration field is given for the slab and cylinder, respectively, by[1]

$$H^* = \begin{cases} 2\pi D J_c/c , & (1) \\ 4\pi R J_c/c . & (2) \end{cases}$$

If a field H is cycled from 0 to H_0 to 0 to $-H_0$, etc., with $H_0 < H^*$, the entire hysteresis loop can be calculated for the slab and cylinder, respectively, by[1]

$$B = HH_0/2H^* \pm (H^2 - H_0^2)/4H^* , \quad (3)$$

$$B = HH_0/H^* \pm (H^2 - H_0^2)/2H^* \pm (H_0^3 - H^2 H_0)/4H^{*2} - (HH_0^2 + H^3/3)/4H^{*2} , \quad (4)$$

where the "plus" and "minus" signs correspond to increasing and decreasing H, respectively.

If $H_0 > H^*$, Eqs. (3) and (4) no longer hold. For $H_0 > H^*$, we extend Bean's analysis to get $B(H)$ for the case of a slab. For H increasing,

$$B = H - H^*/2 + (H + H_0 - 2H^*)^2/4H^* , \quad \text{for } -H_0 < H < -H_0 + 2H^* ,$$

$$B = H - H^*/2, \quad \text{for } -H_0 + 2H^* < H < H_0 ,$$

and for H decreasing , (5)

$$B = H + H^*/2 - (H - H_0 + 2H^*)^2/4H^* \quad \text{for } H_0 > H > H_0 - 2H^* ,$$

$$B = H + H^*/2 \quad \text{for } H_0 - 2H^* > H > -H_0 .$$

For the case of a cylinder, for H increasing,

$$B = H - H^*/3 - (H + H_0 - 2H^*)^3/12H^{*2} \quad \text{for } -H_0 < H < -H_0 + 2H^* ,$$

$$B=H-H^*/3 \quad \text{for } -H_0+2H^*<H<H_0 ,$$

and for H decreasing ,

$$B=H+H^*/3-(H-H_0+2H^*)^3/12H^{*2} \quad \text{for } H_0>H>H_0-2H^* , \tag{6}$$

$$B=H+H^*/3 \quad \text{for } H_0-2H^*>H>-H_0 .$$

Comparing Eqs. (3) and (5) with Eqs. (4) and (6), we see that for both $H_0 \ll H^*$ and $H_0 \gg H^*$, the formulas for the slab and the cylinder are the same except for a prefactor. This is because for any geometry, flux penetrates only the surface area if H_0 is much smaller than H^*, so that the hysteresis is proportional to H_0^2. It is also true that for H_0 much larger than H^*, there is a maximum field that the shielding currents can screen out, corresponding to a flat region in the magnetization. Therefore in the two limiting cases $H_0 \ll H^*$ and $H_0 \gg H^*$, the formulas for the slab should apply to other geometries as well, except for a prefactor. Hence we will focus the remainder of our discussion on the slab case.

Using the nonlinear magnetization given by Eqs. (3)–(6), we can calculate the amplitude of the harmonics generated when an ac magnetic field is applied to a sample. We assume the ac field has the form $H=H_{ac}\cos(\omega t)$. Substituting into Eqs. (3)–(6) and using Fourier analysis, we find

$$B=\sum_n \alpha_n \cos(\omega t)+\sum_n \beta_n \sin(\omega t), \quad n=1,2,3,\ldots , \tag{7}$$

where the coefficients α_n are the in-phase components and β_n are the out-of-phase components. For the slab case with $H_{ac}<H^*$, the results are, as found by Bean,[1]

$$\alpha_1=H_{ac}^2/(2H^*) ,$$

$$\alpha_n=0 \quad (\text{for } n>1) ,$$

$$\beta_n=0 \quad (\text{for even } n) ,$$

$$\beta_n=-(H_{ac}^2/H^*)[2/\pi(n-2)n(n+2)] \quad (\text{for odd } n) . \tag{8}$$

If $H_{ac}>H^*$, we find from our Eq. (5)

$$\alpha_n=\beta_n=0 \quad (\text{for even } n) ,$$

$$\alpha_1=H_{ac}-(4\pi H^*)^{-1}\{(H_{ac}^2/2)[\sin(3X)/3+\sin X]+[H_{ac}^2+2(H_{ac}-2H^*)^2]\sin X-H_{ac}(H_{ac}-2H^*)[\sin(2X)+2X]\} ,$$

$$\beta_1=2H^*/\pi+(4\pi H^*)^{-1}((H_{ac}^2/2)\{[\cos(3X)-1]/3+(1-\cos X)\}$$
$$+[H_{ac}^2+2(H_{ac}-2H^*)^2](\cos X-1)-H_{ac}(H_{ac}-2H^*)[\cos(2X)-1]) , \tag{9}$$

$$\alpha_n=-(4\pi H^*)^{-1}((H_{ac}^2/2)\{\sin[(n+2)X]/(n+2)+\sin[(n-2)X]/(n-2)\}+[H_{ac}^2+2(H_{ac}-2H^*)^2]\sin(nX)/n$$
$$-2H_{ac}(H_{ac}-2H^*)\{\sin[(n+1)X]/(n+1)+\sin[(n-1)X]/(n-1)\}) \quad (\text{for odd } n>1) ,$$

$$\beta_n=2H^*/n\pi+(4\pi H^*)^{-1}[(H_{ac}^2/2)(\{\cos[(n+2)X]-1\}/(n+2)+\{\cos[(n-2)X]-1\}/(n-2))$$
$$+[H_{ac}^2+2(H_{ac}-2H^*)^2][\cos(nX)-1]/n$$
$$-2H_{ac}(H_{ac}-2H^*)(\{\cos[(n+1)X]-1\}/(n+1)$$
$$+\{\cos[(n-1)X]-1\}/(n-1))] \quad (\text{for odd } n>1) ,$$

where

$$X=\cos^{-1}(1-2H^*/H_{ac}), \quad 0<X<\pi .$$

The Bean model predicts that in the slab case for $H_{ac}<H^*$, all odd harmonics are proportional to H_{ac}^2/H^*. For $H_{ac} \gg H^*$, X approaches zero, so that the out-of-phase component β_n approaches $2H^*/n\pi$, while α_n approaches zero.

As already noted, the Bean model (with $J_c=\text{const}$) does not predict the generation of even harmonics even in the presence of an additional dc field. Calculation shows that except for the dc component, the magnetization in the field

$$H=H_{dc}+H_{ac}\cos(\omega t) ,$$

is given by Eqs. (3)–(6) with H replaced by $H-H_{dc}$. Therefore Eqs. (8) and (9) remain valid in the presence of the dc field.

B. Anderson-Kim model

The critical current density in the critical state is determined by the pinning force:

$$\boldsymbol{\alpha}=(1/c)\mathbf{J}_c\times\mathbf{H}_{\text{local}} , \tag{10}$$

where α is the pinning force per unit volume and c is the speed of light. A series of papers by Anderson, Kim, and co-workers[8] indicates that taking α as a constant is a good approximation for many systems, so that

$$J_c=c\alpha/H_{\text{local}} . \tag{11}$$

This leads to a parabolic flux density profile as illustrated in Fig. 1. Here, we discuss only the slab case, although our results hold for other geometries (except for a prefactor) in the limiting cases $H \ll H^*$ and $H \gg H^*$. The penetration field H^* for a slab of thickness D is

$$H^*=(4\pi\alpha D)^{1/2} . \tag{12}$$

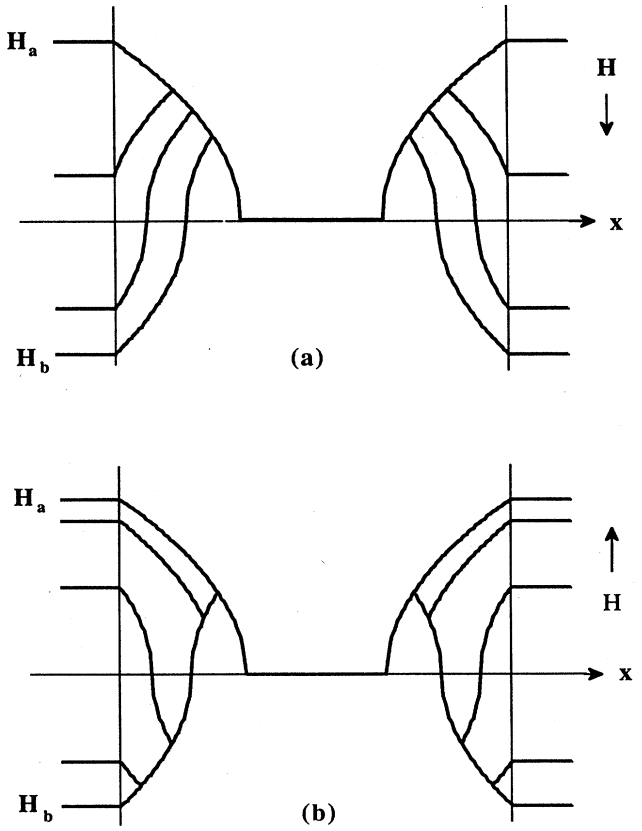

FIG. 1. Flux density profile for an infinitely long slab in a field H cycled between H_a and H_b, where $H_b<0<H_a$, $|H_a|>|H_b|$, and $H_a<H^*$. Vertical axis is local flux density. (a) External field H decreasing from H_a to H_b; (b) H increasing from H_b to H_a.

Now we calculate the magnetization of the superconductor immersed in a field H cycled between H_a and H_b, where $H_a>H_b$. There are two cases depending on whether

$$\Delta^2\equiv[H_a^2\mathrm{sgn}(H_a)-H_b^2\mathrm{sgn}(H_b)]$$

is greater or less than $2H^{*2}$. Here the definition of the function $\mathrm{sgn}(x)$ is given by

$$\begin{aligned}&\mathrm{sgn}(x)=1 \quad \text{if } x>0\ ,\\ &\mathrm{sgn}(x)=-1 \quad \text{if } x<0\ ,\\ &\mathrm{sgn}(x)=0 \quad \text{if } x=0\ .\end{aligned}\tag{13}$$

For the case $\Delta^2>2H^{*2}$, the result is, for H decreasing:

$$B=[2/(3H^{*2})]\{2|[H^2\mathrm{sgn}(H)+H_a^2\mathrm{sgn}(H_a)]/2|^{3/2}-|H|^3-|H^{*2}-H_a^2\mathrm{sgn}(H_a)|^{3/2}\}$$

for

$$H_a>H>|H_a^2\mathrm{sgn}(H_a)-2H^{*2}|^{1/2}\mathrm{sgn}[H_a^2\mathrm{sgn}(H_a)-2H^{*2}],$$

$$B=[2/(3H^{*2})]\{|[H^2\mathrm{sgn}(H)+H^{*2}]|^{3/2}-|H|^3\}$$

for

$$|H_a^2\mathrm{sgn}(H_a)-2H^{*2}|^{1/2}\mathrm{sgn}[H_a^2\mathrm{sgn}(H_a)-2H^{*2}]>H>H_b\ ,$$

and for H increasing, (14)

$$B=-[2/(3H^{*2})]\{2|[H^2\mathrm{sgn}(H)+H_b^2\mathrm{sgn}(H_b)]/2|^{3/2}-|H|^3-|H^{*2}+H_b^2\mathrm{sgn}(H_b)|^{3/2}\}$$

for

$$H_b<H<|H_b^2\mathrm{sgn}(H_b)+2H^{*2}|^{1/2}\mathrm{sgn}[H_b^2\mathrm{sgn}(H_b)+2H^{*2}],$$

$$B=-[2/(3H^{*2})]\{|[H^2\mathrm{sgn}(H)-H^{*2}]|^{3/2}-|H|^3\}$$

for

$$|H_b^2\mathrm{sgn}(H_b)+2H^{*2}|^{1/2}\mathrm{sgn}[H_b^2\mathrm{sgn}(H_b)+2H^{*2}]<H<H_a\ .$$

The other case is $\Delta^2<2H^{*2}$; the result is,

$$B=[2/(3H^{*2})]\{2|[H^2\mathrm{sgn}(H)+H_a^2\mathrm{sgn}(H_a)]/2|^{3/2}-|H|^3-|[H_a^2\mathrm{sgn}(H_a)+H_b^2\mathrm{sgn}(H_b)]/2|^{3/2}\}+B_0$$

for H decreasing from H_a to H_b and (15)

$$B=-[2/(3H^{*2})]\{2|[H^2\mathrm{sgn}(H)+H_b^2\mathrm{sgn}(H_b)]/2|^{3/2}-|H|^3-|[H_a^2\mathrm{sgn}(H_a)+H_b^2\mathrm{sgn}(H_b)]/2|^{3/2}\}+B_0$$

for H increasing from H_b to H_a. B_0, which is the dc component contributed by the inactive interior of the sample [deeper than a distance of $\Delta^2D/(4H^{*2})$ from the surface] that is not reached by the ac field, depends on the initial condition. We plot one example of the flux density profiles in Fig. 1 to indicate how Eqs. (14) and (15) are calculated.

For the special case of symmetric field swings where $H_a=-H_b=H_0$, the preceding results can be simplified. If $H_0<H^*$, we have from Eq. (15)

$$B=\pm(2H_0^3/3H^{*2})\times\{2[(1\pm H/H_0|H/H_0|)/2]^{3/2}-|H/H_0|^3\}\ ,\tag{16}$$

where the plus and minus signs correspond to decreasing and increasing H, respectively.

When a superconductor is immersed in a pure ac field, i.e., $H=H_{ac}\cos(\omega t)$, we have $H_a=-H_b=H_0=H_{ac}$. If $H_{ac}<H^*$, the harmonic signal is proportional to H_{ac}^3/H^{*2} which is the prefactor in Eq. (16). The other case $H_{ac}>H^*$ is a little more complicated, since Eq. (14) cannot be simplified into a single equation. However, in the extreme case $H_{ac}\gg H^*$, we find the harmonic signal to be approximately proportional to H^{*2}/H_{ac}. These results differ from the Bean model results quoted after Eq. (9).

As pointed out in the beginning of Sec. III, only odd harmonics exist in zero dc field, while even harmonics appear in a dc field. If we assume the external field has the form $H=H_{dc}+H_{ac}\cos(\omega t)$, the Anderson-Kim model results Eqs. (14) and (15) can be used to study the magneti-

zation and harmonic generation. Here $H_a = H_{dc} + H_{ac}$ and $H_b = H_{dc} - H_{ac}$. We notice that $\Delta^2 > 2H^{*2}$, which is the condition for Eq. (14), is always satisfied if $H_{ac} > H^*$. Also, for a given dc field, we have to switch from Eq. (14) to Eq. (15) as the ac field is decreased, since $\Delta^2 < 2H^{*2}$ is always satisfied when $H_{ac} \ll H^*$.

Now we let the external field

$$H = H_{dc} + H_{ac}\cos(\omega t) ,$$

and use Fourier analysis to write the field $B(t)$ from Eq. (14) and Eq. (15) as

$$B(t) = \sum_n \alpha_n \cos(n\omega t) + \sum_n \beta_n \sin(n\omega t) + \beta_0 ,$$
$$n = 1, 2, 3, \ldots , \tag{17}$$

where β_0 is the dc component and the coefficients α_n and β_n are given by the Fourier integrals:

$$\alpha_n = \frac{1}{\pi}\int_{-\pi}^{\pi} B(t)\cos(n\omega t)d(\omega t) , \tag{18}$$

$$\beta_n = \frac{1}{\pi}\int_{-\pi}^{\pi} B(t)\sin(n\omega t)d(\omega t) . \tag{19}$$

The magnitude of the nth harmonic B_n is then equal to $(\alpha_n^2 + \beta_n^2)^{1/2}$. The integrations for α_n and β_n were done numerically. Figure 2 is a plot of the harmonic signal B_n as a function of applied dc field for various harmonic numbers n for the case $\Delta^2 < 2H^{*2}$, calculated from Eq. (15). For fixed H_{dc}/H_{ac}, B_n scales with H_{ac}^3, but these curves are universal as long as $\Delta^2 < 2H^{*2}$. Clearly, even harmonics are nonzero for $H_{dc} \neq 0$. As shown in Fig. 2, we also find that in the region $H_{dc} < H_{ac}$, the nth harmonic signal has an oscillatory dependence on H_{dc}/H_{ac}.

When $H_{ac} > H^*$, harmonic signals in the presence of a dc field are given by the Fourier transformation of Eq. (14), and the results depend on the parameter H_{ac}/H^*. However, when H_{ac}/H^* is very large, this dependence only changes the absolute value of the harmonic signal rather than the overall structure. Figure 3(a) is a plot of the numerically calculated result with $H_{ac} = 10H^*$. The regular oscillating structure is apparent, with a quasi-period of oscillation $\delta H_{dc} \approx \pi H_{ac}/n$.

A simple argument can be made to explain the above oscillating structure when $H_{dc}/H_{ac} < 1$ for the case of large H_{ac}/H^*. In Fig. 4, we plot the magnetization $M(t)$ as a function of time, for a sample in the field

$$H = H_{dc} + H_{ac}\cos(\omega t) ,$$

with $\omega = 1$, $H_{dc} = 5H^*$, and $H_{ac} = 10H^*$, for $-\pi < t < \pi$. The plots are from the Bean model and the Anderson-Kim model, respectively. It is clear that the Bean model

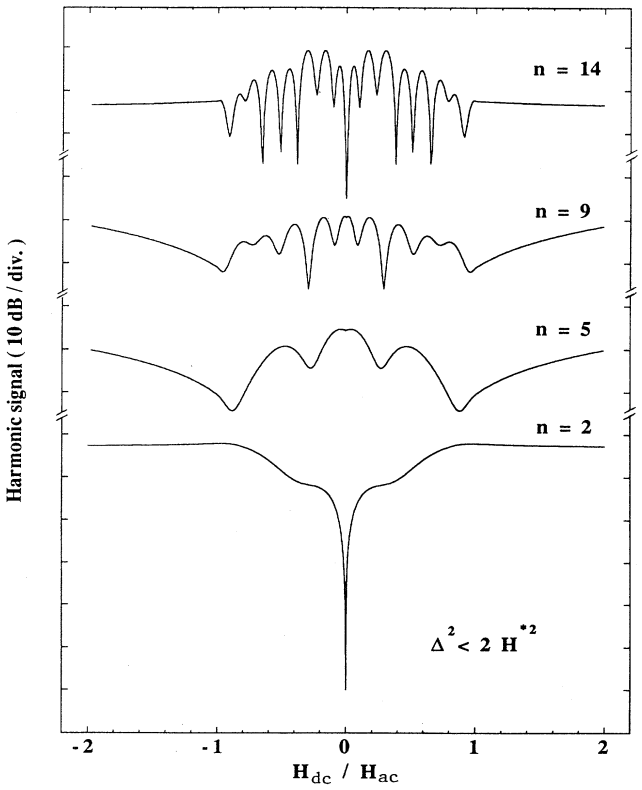

FIG. 2. Harmonic signal numerically calculated from the Anderson-Kim model as a function of applied dc field for various harmonic numbers n, where $\Delta^2 < 2H^{*2}$.

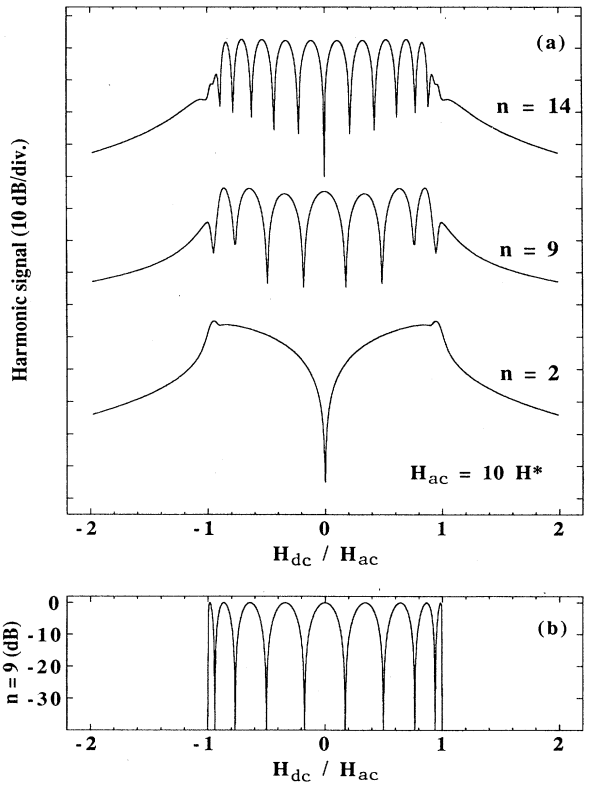

FIG. 3. (a) Harmonic signal numerically calculated from the Anderson-Kim model as a function of applied dc field for various harmonic numbers n, where $H_{ac} = 10H^*$; (b) ninth harmonic signal vs H_{dc}/H_{ac} as given by the approximation Eq. (20).

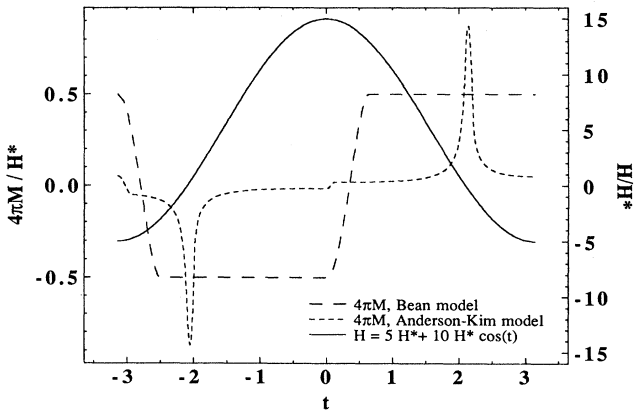

FIG. 4. Magnetization as a function of time t, $-\pi < t < \pi$, in external field $H = 5H^* + 10H^*\cos(t)$, as predicted by the Bean model and Anderson-Kim model.

$M(t)$ has flat regions and is not sensitive to $H(t)$, while the Anderson-Kim model shows two peaks in $M(t)$ when $H(t) \approx 0$. We argue that the contribution from these two peaks is the physical reason for the oscillation of the harmonic amplitudes, since $M(t)$ elsewhere is much smaller and slowly varying, and for high n largely cancels out when multiplied by $\cos(n\omega t)$ and $\sin(n\omega t)$ in the Fourier integration. For simplicity, we use δ functions to represent the magnetization, so that $M(H) \sim \pm\delta(H)$, where "+" and "−" signs are for decreasing and increasing H, respectively. Therefore

$$M(t) \sim \pm\delta(H_{dc} + H_{ac}\cos(\omega t)) .$$

For $|H_{dc}/H_{ac}| < 1$, $M(t)$ has a nonzero value only at $\omega t = \cos^{-1}(-H_{dc}/H_{ac})$ and $\omega t = -\cos^{-1}(-H_{dc}/H_{ac})$. Therefore for $|H_{dc}| < H_{ac}$, the in-phase component α_n and the out-of-phase component β_n of the nth harmonic signal can be approximated by

$$\begin{aligned} \alpha_n &\sim \{\cos[n\cos^{-1}(-H_{dc}/H_{ac})] \\ &\quad -\cos[-n\cos^{-1}(-H_{dc}/H_{ac})]\} \\ &\sim 0 , \\ \beta_n &\sim \{\sin[n\cos^{-1}(-H_{dc}/H_{ac})] \\ &\quad -\sin[-n\cos^{-1}(-H_{dc}/H_{ac})]\} \\ &\sim 2\sin[n\cos^{-1}(-H_{dc}/H_{ac})] . \end{aligned} \tag{20}$$

Since

$$\cos^{-1}(x) \approx \pi/2 - x$$

for small x, the nth harmonic signal has a quasiperiod of oscillation $\delta H_{dc} \approx \pi H_{ac}/n$. In Fig. 3(b), we plot the ninth harmonic signal predicted by Eq. (20). Note the similarity between the periodicities of this approximation and that of the exact calculation for $n = 9$ plotted in Fig. 3(a).

When H_{dc} is much larger than H_{ac}, J_c is predominantly determined by H_{dc}. Thus for the entire subloop of magnetization, J_c is approximately constant for any given dc field. In this region, the results of the Anderson-Kim model converge to those of the Bean model. In particular, the Anderson-Kim model predicts that the even harmonics disappear for $H_{dc} \gg H_{ac}$.

IV. COMPARISON OF EXPERIMENTAL RESULTS WITH THEORY

A. Hysteresis loops and harmonics versus ac field

We measured the magnitude of the odd harmonics as a function of H_{ac} with zero dc field in both powder and bulk samples. Since the results depend on the sample geometry, we focused our measurements on thin slab samples and compared our results with those predicted earlier by the critical-state model for a slab geometry. Our samples fall into two categories: (1) samples with small H^* (comparable to the measuring magnetic field), and (2) samples with high H^* (much larger than the fields used in our experiments).

Most samples in the first category are degraded bulk samples with very small penetration fields H^* (about 1 Oe), though similar results can be seen in powders. Since H^* is very small, we are able to see the predicted saturation of harmonic amplitude as H_{ac} exceeds H^*. At smaller H_{ac}, the third harmonic signal is proportional to $(H_{ac})^{\nu}$, with ν observed to be between 1.5 and 2, while the Bean model predicts $\nu = 2$ for $H_{ac} < H^*$. This deviation may be attributed to a decrease in the demagnetization effect as flux penetrates deep into the sample. For $H_{ac} > H^*$, we observe that the harmonic signal approaches a constant as predicted by the Bean model.

We also measured hysteresis loops for our degraded samples at various H_{ac}, as shown in Figs. 5(a)–5(c). We observe that a flat region emerges and increases in width as we increase H_{ac}. Figs. 5(d)–5(f) show a fit for several values of H_{ac}/H^* using the formula

$$4\pi M = 4\pi M_{Bean} - aH ,$$

where $a = 0.3$ and

$$4\pi M_{Bean} = B_{Bean} - H$$

is given by Eqs. (3) and (5). The aH term accounts for the diamagnetism of grains which are still in the Meissner state (since H_{c1g} is about 60 Oe), even if flux is penetrating *between* the grains. For granular superconductors, a is expected to be less than one, as noted by Clem and Kogan.[11] There is good agreement between the experimental results and this theoretical model. Estimating that $H^* = 0.6$ Oe for a degraded sample with a thickness of about 4 mm, the critical current density is approximately 2.4 A/cm^2.

The samples in the second category were the standard ones with large H^*, for which the available measuring ac fields were always less than H^*. Figure 6 shows the third harmonic signal as a function of H_{ac}. Since we find that the harmonic signal continues to rise steeply for H_{ac} up to 12 Oe, which is the maximum ac field used in our experiments, H^* must be larger than 12 Oe although we

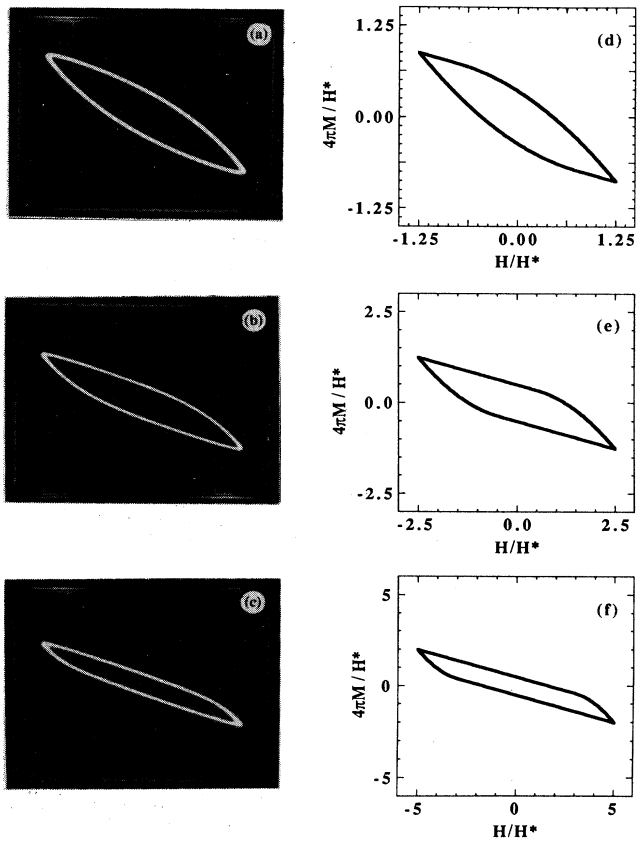

FIG. 5. (a)–(c) Hysteresis loops measured at 77 K in a bulk sample of Y-Ba-Cu-O with small H^* (degraded sample) for various H_{ac}: (a) $H_{ac}=0.7$ Oe, y axis: 5 mV/div.; (b) $H_{ac}=1.4$ Oe, y axis: 10 mV/div.; (c) $H_{ac}=2.8$ Oe, y axis: 20 mV/div. (d)–(f) Hysteresis loops predicted by the formula $4\pi M=4\pi M_{\text{Bean}}-0.3H$: (d) $H_{ac}=1.25H^*$, (e) $H_{ac}=2.5H^*$, (f) $H_{ac}=5H^*$.

could not determine its value exactly. This minimum value for H^* corresponds to a critical current density of 2×10^2 A/cm^2 for a 1-mm thick sample. Since the measuring field was probably much less than H^*, the flux only penetrated near the surface. Thus the demagnetization coefficient, which is small in any case due to the thin slab geometry, remains more or less constant when we change the field.

As shown in Fig. 6, for small H_{ac}, we find that the third harmonic is proportional to H_{ac}^2, corresponding to the Bean model. For larger H_{ac} (>3 Oe), we find that the third harmonic is proportional to H_{ac}^3, corresponding to the Anderson-Kim model. When H_{ac} crosses over from the Bean regime to the Anderson-Kim regime, the generation of even harmonics becomes observable.

B. Harmonic amplitude versus temperature

We measured the temperature dependence of the third harmonic signal in constant ac fields (with $H_{dc}=0$) in both bulk and powder samples, as shown in Fig. 7(a). For an ac drive field with a constant amplitude of 5 Oe, a

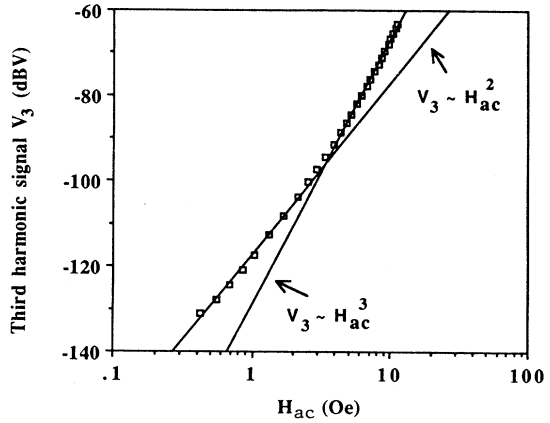

FIG. 6. Third-harmonic signal measured at 77 K in a bulk sample of Y-Ba-Cu-O with large H^* ($\gg H_{ac}$) as a function of H_{ac}.

peak in harmonic amplitude near the transition temperature is observed in our bulk samples but not in our powder samples. This feature can be understood in the general framework of the Bean model as follows. (The same qualitative result can be obtained from the Anderson-Kim model.) Assume we have $H_{ac}<H^*$ at

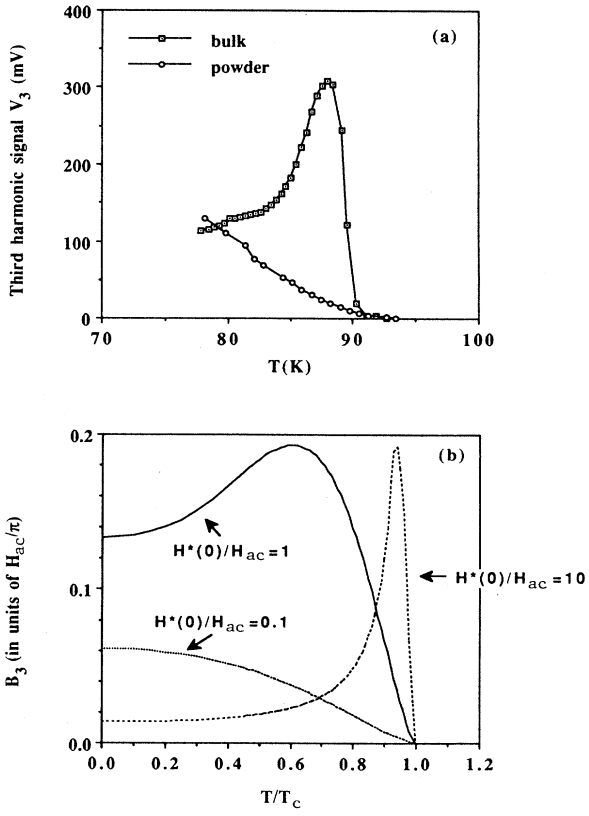

FIG. 7. (a) Third-harmonic signal as a function of temperature measured in bulk and powder samples of Y-Ba-Cu-O, $H_{ac}=5$ Oe; (b) theoretical temperature dependence of the third-harmonic signal for various values of $H^*(0)/H_{ac}$.

some lower temperature where J_c is large. As the temperature increases, the harmonic amplitude V_n, which as shown in Eq. (8) is proportional to the inverse of H^* and therefore the inverse of J_c, should increase since J_c decreases with increasing temperature. But as the temperature approaches T_c, the critical current becomes very small causing H^* to become much smaller than H_{ac}, so that V_n becomes proportional to H^*, as indicated by Eq. (9). As a result, V_n should decrease with $J_c(T)$ near T_c, and we should expect a peak somewhere near the transition temperature. However, there is no peak if H^* at zero temperature is still smaller than H_{ac}. If we assume the critical current has the two-fluid temperature dependence

$$[1-(T/T_c)^2][1-(T/T_c)^4]^{1/2} ,$$

we can use Eqs. (8) and (9) to predict the temperature dependence of the harmonics. Figure 7(b) shows a plot of the resulting predicted temperature dependence of the third harmonic component for various $H^*(T=0)/H_{ac}$. For large $H^*(T=0)/H_{ac}$, the peak is very close to T_c. For smaller $H^*(T=0)/H_{ac}$, the peak occurs at lower temperatures, finally disappearing for $H^*(T=0)/H_{ac}$ smaller than 0.58 [see the following]. In our experiments, powder samples with small H^* (small particle sizes) do not show peaks, while bulk samples with much larger H^* show definite peaks near T_c, as expected from this model.

The peak occurs at the temperature where

$$(\partial B_n/\partial T)_{H_{ac}}=(\partial B_n/\partial H^*)_{H_{ac}}(dH^*/dT)=0 . \quad (21)$$

Since H^* decreases monotonically as temperature increases, (dH^*/dT) is always nonzero. Substituting $B_{n=3}$, given by Eq. (9), into Eq. (21), we find

$$H^*(T_{peak})\approx 0.58 H_{ac}$$

for the third harmonic signal for the slab case of the Bean model. The Anderson-Kim model predicts a similar result.

Shaulov and Dorman[5] reported measurements of the third harmonic amplitude in very small constant ac fields as a function of temperature for various dc fields ranging form 0 to 1 kOe. As they increased the dc field, the peak moved to lower temperatures. This is consistent with the results of our critical-state model since H^*, proportional to J_c, decreases as the dc field is increased. We also note that a similar temperature dependence for the peaks in the out-of-phase component of the ac susceptibility has been reported by various experimental groups.[12]

C. Harmonic amplitude versus harmonic number *n*

Figure 8 shows the magnitudes of the nth harmonic signals as a function of (odd) n measured in a thin slab of Y-Ba-Cu-O ($13.6\times10\times1.6$ mm^3) at various ac field amplitudes (in zero dc field). The ac fields used in the measurements were always smaller than the penetration field H^* of the sample, i.e., $H_{ac}<H^*$. The surface of the sample was sanded before making the measurements to minimize the effect of bad surfaces. The solid line is the Bean

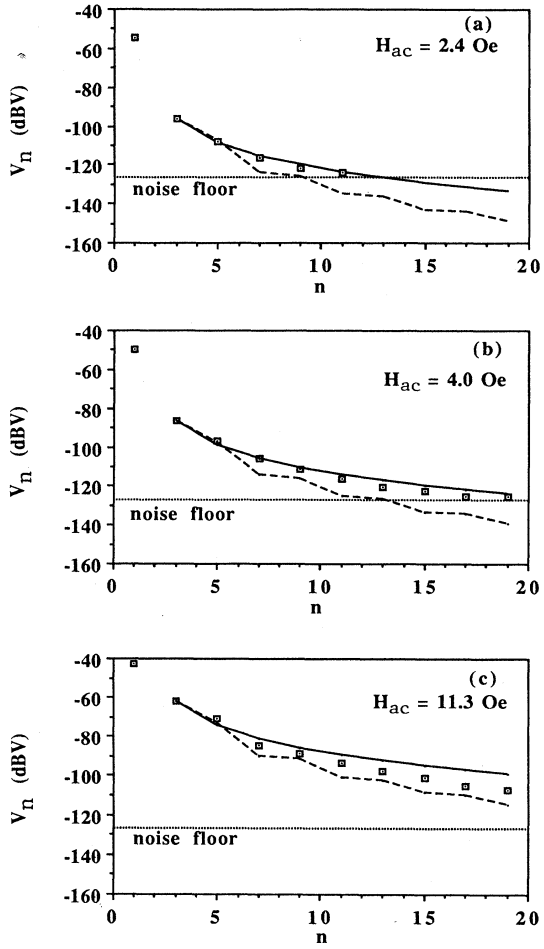

FIG. 8. Magnitude of nth harmonic signal as a function of n for various H_{ac} in a thin slab sample of Y-Ba-Cu-O at 77 K, $f=5$ kHz, $H_{dc}=0$: (a) $H_{ac}=2.4$ Oe, (b) $H_{ac}=4.0$ Oe, (c) $H_{ac}=11.3$ Oe. Dots: experimental data; solid line: Bean model, $H_{ac}<H^*$; dashed line: Anderson-Kim model, $H_{ac}<H^*$. Fits are scaled to third-harmonic amplitude.

model prediction when $H_{ac}<H^*$, given by Eq. (8), and the dashed line is the Anderson-Kim model prediction when $H_{ac}<H^*$, numerically calculated from the Fourier transformation of Eq. (16). Both of these curves are scaled to fit the third harmonic signal. For small H_{ac}, the power spectrum is very close to that predicted by the Bean model. But as the ac field amplitude is increased, the spectrum deviates from the Bean model and moves toward that which is predicted by the Anderson-Kim model, corresponding to a crossover from one model to the other. In order to accurately predict the crossover, a more realistic model such as one based on $J_c=c\alpha/(H+H_\mu)$ would be necessary, where H_μ is a material-dependent parameter characterizing the crossover.

We notice that the crossover field in Fig. 8 appears to be of the order of 10 Oe, while the crossover field for the third harmonic signal shown in Fig. 6 appears to be around 3–4 Oe, even though the measurements were

done on the same sample. The reason for this difference is not quite clear. However, since the theoretical line for the Anderson-Kim model is lower relative to that of the Bean model for the higher harmonics, the lower harmonics must change faster and hence must change first in the transition from the square to the cubic dependence on H_{ac}. Therefore it is plausible that the third harmonic signal would cross over first as H_{ac} increases.

D. Harmonic amplitude versus dc field

We also measured the even harmonic signals as a function of dc field. We observed a very sharp dip in the second harmonic amplitude at $H=0$ due to the restoration of the broken symmetry of the hysteresis loop. Figure 9 is a plot of our experimental results and a prediction by the Anderson-Kim model. Due to the limitations of our present setup, we could only measure harmonics in H_{dc} up to 0.4 H_{ac}, and hence we were not able to verify all the theoretical results shown in Figs. 2 and 3 for the bulk slab sample.

Jeffries *et al.*[4] have reported structures similar to those shown in Fig. 3(a) measured in powder samples in ac fields larger than 10 Oe. Though the measurements were from powder samples which should fit our slab results only qualitatively, the measured spacing between minima shown in Fig. 5 of Ref. 4 is very close to $\pi H_{ac}/n$, as predicted by our critical-state model. These structures are understood as resulting from a symmetry-breaking process.

E. Effect of sample thickness

One bulk piece was cut into several smaller samples of the same length and width but different thicknesses. The third-harmonic signals measured in these samples in zero dc field were found to be more or less independent of sample thickness. This is consistent with the critical state model so long as $H_{ac}<H^*$. The nth harmonic component of the magnetization, B_n, is proportional to the inverse of sample thickness in the regime $H_{ac}<H^*$, according to Eqs. (8) and (2) of the Bean model or Eqs. (16) and (12) of the Anderson-Kim model. Since the harmonic signals in the secondary coil voltage output are proportional to B_n times the sample volume, they are independent of sample thickness. Stated more physically, the measured signal comes from a surface layer penetrated by the field, which is independent of the thickness of the inactive material between the two surface layers.

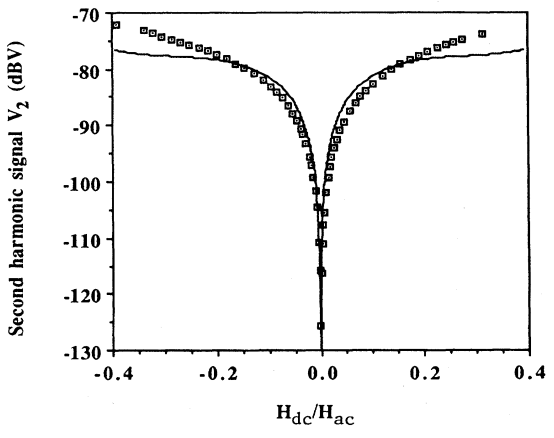

FIG. 9. Second-harmonic power as a function of H_{dc}/H_{ac}. Solid line calculated from the Anderson-Kim model with $\Delta^2<2H^{*2}$. Dots are measured in a Y-Ba-Cu-O bulk sample at 77 K with $H_{ac}=4.75$ Oe.

V. COMPARISON WITH OTHER MODELS

The critical-state model just presented deals with macroscopic current flowing through an effective medium. Previous attempts to explain harmonic generation in high-temperature superconductors have relied on simple network pictures involving Josephson junctions and inductive loops.[2–5] The formula that results in the inverse-Josephson-effect model[2] appears to be mathematically equivalent to the single-loop formula used in the loop model.[3,4] We will focus our discussion on the differences between the loop model proposed by Jeffries *et al.*[3,4] and the critical state model proposed in this paper, and compare the predictions of both models with the experimental observations.

First, the temperature dependence of the harmonic amplitude in the loop model is basically the same as that of the critical current. Therefore no peak in the harmonic amplitude as a function of temperature is predicted by the loop model. The temperature-dependence measurements were done with powders in the work of Jeffries *et al.*, yielding results which seemed to be consistent with their theory. The same proportionality to J_c is obtained from the critical state model, if the value of H^* is much smaller than the measuring ac fields, as is the case with our powder samples. However, our critical-state model predicts that the temperature dependence of the harmonics is a function of $H^*_{(T=0)}/H_{ac}$ and that a peak appears if $H^*_{(T=0)}/H_{ac}$ is greater than ~ 1, as supported by our experimental results from bulk samples. These features cannot be explained by the loop model because it neglects macroscopic shielding effects.

To explain why the spacing between minima of the nth harmonic amplitude as a function of dc field is proportional to H_{ac}/n, it is suggested in Ref. 4 that the effective loop area is proportional to H_{ac}, but no clear justification is given. It follows naturally from our model that the spacing δH_{dc} is $\pi H_{ac}/n$ for small H_{dc}/H_{ac} when $H_{ac}>H^*$, which appears to explain the measured results.

The harmonic signal in zero dc field as a function of H_{ac} is not discussed quantitatively in earlier work while we observe experimentally and describe theoretically the behavior corresponding to a crossover from the Bean regime to the Anderson-Kim regime.

The dependence on the harmonic number n is described by our model quantitatively for small H_{ac}, i.e., the Bean regime, and qualitatively for large H_{ac}, i.e., the Anderson-Kim regime. The loop model only qualitative-

ly describes this dependence.

The critical-state model has been used successfully to describe magnetization in hard superconductors for the past twenty-five years, and it describes many other experimental results in high-temperature superconductors.[10] Given its simplicity and agreement with a broader range of experimental results, the critical-state model seems to be a preferable explanation for harmonic generation compared to the loop model which involves new assumptions of uncertain applicability.

VI. CONCLUSIONS

The critical-state model appears to account for all experimental results on low frequency harmonic generation in Y-Ba-Cu-O samples without the *ad hoc* assumptions of other models. Since the fields used in our experiments were rather small, we could only probe properties related to the intergranular critical current density and not the intragranular critical current density. However, the same physics probably applies to both situations.

A theoretical limitation of the critical-state model may result if the actual vortex state in high-temperature superconductors is some sort of melted or liquid state instead of the conventional rigid Abrikosov lattice, as has been proposed by Nelson.[13] For a complete analysis of such a case, the critical-state model would have to be modified to take into account explicitly the time-dependent relaxation effects.

After this manuscript was completed, we became aware of the work of Müller *et al.*,[14] which also applies a critical-state model to interpret harmonic generation in Y-Ba-Cu-O and reaches similar conclusions concerning the role of a dc magnetic field.

ACKNOWLEDGMENTS

This work was supported in part by National Science Foundation Grant Nos. DMR-86-14003 and DMR-84-04489, U.S. Office of Naval Research Grant No. N00014-89-J-1565, and U.S. Joint Services Electronics Program (JSEP) Grant No. N10014-89-J-1023.

[1]Charles P. Bean, Rev. Mod. Phys. **36**, 31 (1964).

[2]O. V. Abramov, G. I. Leviev, V. G. Pogodsov, and M. R. Trunin, Pis'ma Zh. Eksp. Teor. Fiz. **46**, 433 (1987) [JETP Lett. **46**, 546 (1987)].

[3]Carson Jeffries, Q. Harry Lam, Youngtae Kim, L. C. Bourne, and A. Zettl, Phys. Rev. B **37**, 9840 (1988); Q. Harry Lam and Carson Jeffries, *ibid.* **39**, 4772 (1989).

[4]C. D. Jeffries, Q. H. Lam, Y. Kim, C. M. Kim, A Zettl, and M. P. Klein, Phys. Rev. B **39**, 11 526 (1989).

[5]A. Shaulov and D. Dorman, Appl. Phys. Lett. **53**, 2680 (1988).

[6]L. Ji, R. H. Sohn, G. C. Spalding, C. J. Lobb, M. Tinkham, and Z. X. Zhao, Bull. Am. Phys. Soc. **34**, 602 (1989).

[7]T. Xia and D. Stroud, Phys. Rev. B **39**, 4792 (1989).

[8]Y. B. Kim, C. F. Hempstead, and A. R. Strnad, Phys. Rev. **129**, 528 (1963); P. W. Anderson and Y. B. Kim, Rev. Mod. Phys. **36**, 39 (1964).

[9]$YBa_2Cu_3O_{7-y}$ powders from W. R. Grace & Co., Davison Chemical Division, P. O. Box 2117, Baltimore, MD 21203.

[10]M. Tinkham and C. J. Lobb, *Solid State Physics* (Academic, San Diego, 1989), Vol. 42, pp. 91–134.

[11]J. R. Clem and V. G. Kogan, Jpn. J. Appl. Phys. **26**, Suppl. 26–3, 1161 (1987).

[12]For example, Y. Oda, I. Nakada, T. Kohara, and K. Asayama, Jpn. J. Appl. Phys. **26**, L608 (1987).

[13]David R. Nelson, Phys. Rev. Lett. **60**, 1973 (1988).

[14]K.-H. Müller, J. C. Macfarlane, and R. Driver, Physica C **158**, 366 (1989).

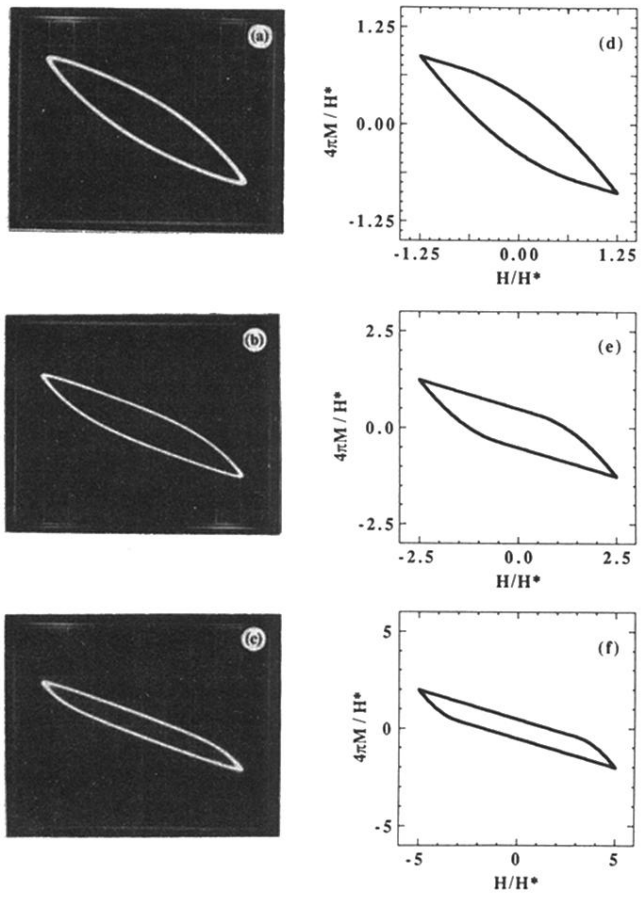

FIG. 5. (a)–(c) Hysteresis loops measured at 77 K in a bulk sample of Y-Ba-Cu-O with small H^* (degraded sample) for various H_{ac}: (a) $H_{ac}=0.7$ Oe, y axis: 5 mV/div.; (b) $H_{ac}=1.4$ Oe, y axis: 10 mV/div.; (c) $H_{ac}=2.8$ Oe, y axis: 20 mV/div. (d)–(f) Hysteresis loops predicted by the formula $4\pi M=4\pi M_{\text{Bean}}-0.3H$: (d) $H_{ac}=1.25H^*$, (e) $H_{ac}=2.5H^*$, (f) $H_{ac}=5H^*$.